Measurements of spin dependent structure function $g_1^d(x, Q^2)$ at COMPASS

Helena Santos, on behalf of the COMPASS Collaboration
LIP - Laboratório de Instrumentação e Física Experimental de Partículas
Av. Elias Garcia, 14, 1000-149, Lisboa, Portugal

Abstract

The COMPASS experiment at the CERN SPS measures the spin dependent structure function g_1^d of the deuteron. Results obtained in the kinematic ranges $Q^2 < 1$ (GeV/c)^2 and $0.0005 < x < 0.02$, as well as $1 < Q^2 < 100$ (GeV/c)^2 and $0.004 < x < 0.7$ are presented. The results of a global QCD fit at Next-to-Leading Order to the world g_1 data are discussed.

1 Introduction

The history of the spin structure of the nucleon begun more than 30 years ago with polarised deep inelastic scattering measurements at SLAC [1]. At that time the quark-parton model has predicted that 60% of the nucleon spin was entirely given by the u and d quarks [2]. The validity of this prediction has been supported by the poor x range of the experiment ($x > 0.1$). Then the EMC collaboration extendend the measurements to $x > 0.01$ and came out with the unexpected value of $0.12 \pm 0.09 \pm 0.14$ [3]. Such a result motivated a set of experiments covering different x ranges at CERN [4], SLAC [5, 6, 7, 8], DESY [9] and JLAB [10]. All these experiments confirmed the small contribution of the quarks (about 20–30%), and thus more contributions are necessary. For a nucleon with +1/2 helicity one should have the sum rule:

$$S_n = \frac{1}{2} = \frac{1}{2}\Delta\Sigma + \Delta G + L_q + L_G \quad (1)$$

where $\Delta\Sigma$ stands for the contribution from the quarks ($\Delta\Sigma = \Delta u + \Delta d + \Delta s$), ΔG is the contribution of the gluons and $L_{q,G}$ are their angular orbital momenta.

This article reports on the experimental procedure to measure the spin-dependent structure function, g_1, at the COMPASS experiment. A NLO QCD analysis performed in order to obtain $\Delta\Sigma$ and an indirect measurement of ΔG is described.

2 Experimental Procedure

COMPASS makes use of the CERN-SPS facilities, impinging a high intensity 160 GeV muon beam on a ^{6}LiD polarised target. Besides the scattered muon, other particles produced in deep inelastic scattering are detected in a two-stage spectrometer. Data presented in this article have been collected in the years 2002, 2003 and 2004, corresponding to an integrated luminosity of about 2 fb^{-1}.

The target consists in two 60 cm long cells, with 3 cm diameter and separated by 10 cm. They are located inside a superconducting solenoid magnet that provides a field of 2.5 T along the beam direction. The maximum angle of aperture provided by the solenoid is 70 mrad [1]. The two cells are oppositely polarised by dynamic nuclear polarisation (DNP), so that the deuteron spins are parallel (↑↑) or antiparallel (↑↓) to the spins of the incoming muons. The polarisations of the two cells are inverted every 8 hours by rotating the magnetic field direction. In this way, acceptances do cancel out in the asymmetry calculation, provided that the acceptance ratios remain unchanged after field rotation. Eventual systematic effects related to the magnetic field do cancel out as well, by reversing the polarisation of each target cell, by DNP, at least once per running period. The two spectrometers (Large Angle Spectrometer (LAS) and Small Angle Spectrometer (SAS)) are located around two dipole magnets, SM1 and SM2. Scintillating fibres and silicon detectors ensure tracking in the beam region, complemented by MicroMeGas and GEM detectors up to 20 cm from the beam. Drift chambers, multi-wire proportional chambers and straw tubes cover both LAS and SAS spectrometers. Electromagnetic and hadronic calorimeters are integrated in both spectrometers. A Ring Imaging Čerenkov Detector separates kaons from pions with momentum up to 43 GeV/c [2]. The COMPASS data acquisition system is triggered by coincidence signals in hodoscopes. Inclusive triggers require the detection of the scattered muon, while semi-inclusive triggers are based on the muon energy loss and on the presence of a hadron signal in the calorimeters. Purely calorimetric triggers are based on the energy deposit in the hadron calorimeter without any condition on the scattered muon. Triggers due to halo muons are eliminated by veto counters installed upstream from the target. The detailed description of the spectrometer can be found in Ref. [11)].

3 The A_1^d Asymmetries

In order to have access to the spin-dependent structure function, g_1^d, the longitudinal photon-deuteron asymmetry, A_1^d, has to be evaluated. In the framework of the quark parton model this quantity can be directly related to the quarks

[1]From the run of 2006 on, COMPASS has a new magnet providing an acceptance a factor 2.5 higher and 3 cells target.

[2]This detector has not been used in the presented analysis.

polarisation via

$$A_1 = \frac{(\sigma_{\gamma\mu}^{\uparrow\downarrow} - \sigma_{\gamma\mu}^{\uparrow\uparrow})}{(\sigma_{\gamma\mu}^{\uparrow\downarrow} + \sigma_{\gamma\mu}^{\uparrow\uparrow})} \simeq \frac{\sum_q e_q^2(\Delta q + \Delta\bar{q})}{\sum_q e_q^2(q + \bar{q})} \tag{2}$$

The starting point for the A_1^d asymmetry extraction is to count the events detected in each target cell, $N_i = a_i \phi_i n_i \sigma_0 (1 + P_B P_T f D A_1^d)$, where a_i is the acceptance of the target cell i, ϕ_i is the incoming muon flux, n_i is the number of target nucleons, σ_0 is the muon-deuteron unpolarised cross-section, P_B and P_T are the beam and target polarisations and f and D are the dilution and depolarisation factors, respectively. The ratio $(N_1 N_2')/N_2 N_1')$, where N_i' stands for the number of events after magnetic field rotation, relates to A_1^d through a second order equation, in which the fluxes ϕ_i cancel out by ensuring equal muon fluxes for both target cells. The ratio of acceptances does cancel out as well, if $a_1/a_2 = a_1'/a_2'$. In order to minimize the statistical error of the asymmetry, each event is weighted by the product of the dilution and depolarisation factors and the beam polarisation. As the target polarisation is time dependent it is taken as the average value of the run, instead.
Figure 1 shows A_1^d as a function of x for quasi-real photon interactions for the data collected in the years 2002 and 2003. Events are selected by cuts on the four-momentum transfer squared ($Q^2 < 1\,(\mathrm{GeV}/c)^2$) and the fractional energy of the virtual photon ($0.1 < y < 0.9$). Such a kinematic window allows a wide Bjorken scaling variable interval, $0.0005 < x < 0.02$. Furthermore, strict quality criteria are applied to data ensuring that events originate in the target, preventing fake triggers and demanding equal muon fluxes on the two target cells. 280 million events have been analysed corresponding to an integrated luminosity of about 1 fb^{-1}. The asymmetry is compatible with 0 over the whole x range. The error bars are statistical and the grey band corresponds to the systematic errors, which are due to false asymmetries mainly. Details on this analysis can be found in [12].

Figure 2 shows A_1^d as a function of x for DIS events ($Q^2 > 1\,(\mathrm{GeV}/c)^2$), as measured by COMPASS using 2002, 2003 and 2004 data [13]. One should bear in mind that, although part of the x domain ($0.004 < x < 0.7$) is the same of the low Q^2 events, this plot refers to different physics [12]. After data selection 89×10^6 events are available for analysis. The results of the SMC [4], E143 [6], E155 [8] and HERMES [14] experiments, are also shown. The asymmetry is 0 for $x < 0.05$ and becomes larger as x increases, reaching 60% at $x \simeq 0.7$.

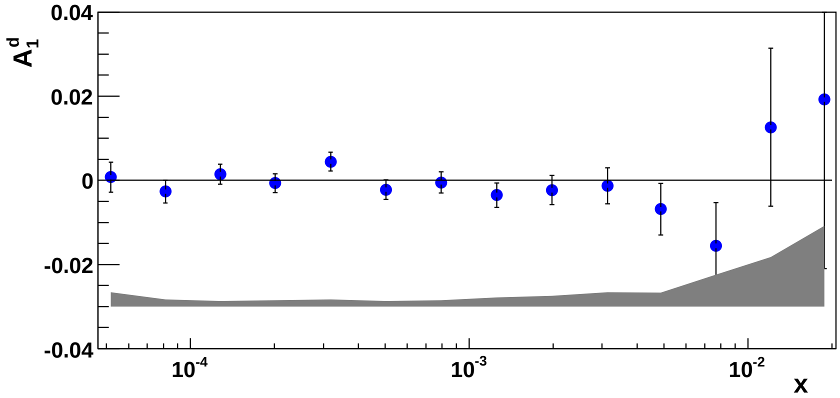

Figure 1: *The asymmetry $A_1^d(x)$ for quasi-real photons($Q^2 < 1$ $(GeV/c)^2$) as a function of x. The errors bars are statistical. Grey band shows the systematic errors.*

The agreement is very good between the different data sets. It should be noted that only COMPASS and SMC were able to measure this asymmetry at very low x, the COMPASS results being essential to disentangle the A_1^d behaviour at $x < 0.03$. Error bars are statistical and the grey band corresponds to the systematic errors of the COMPASS measurements, whose sources come from the uncertainty on beam and target polarisations (5%), dilution factor (6%) and depolarisation factor (4-5%). Radiative corrections and neglecting the transverse asymmetry A_2 are found to have a small effect. The upper limit for the systematic error due to false asymmetries is half of the statistical one.

4 The g_1^N Structure Function

The spin-dependent structure function of the nucleon, $g_1(x)$, is obtained from $A_1(x)$ and the spin-independent structure function $F_2(x)$ through

$$g_1(x) = A_1(x)\frac{F_2(x)}{2x(1+R)} \ . \tag{3}$$

Figure 3 shows g_1^d as a function of x for quasi-real photon interactions. g_1^d is found to be consistent with 0 in the investigated x range. The statistical

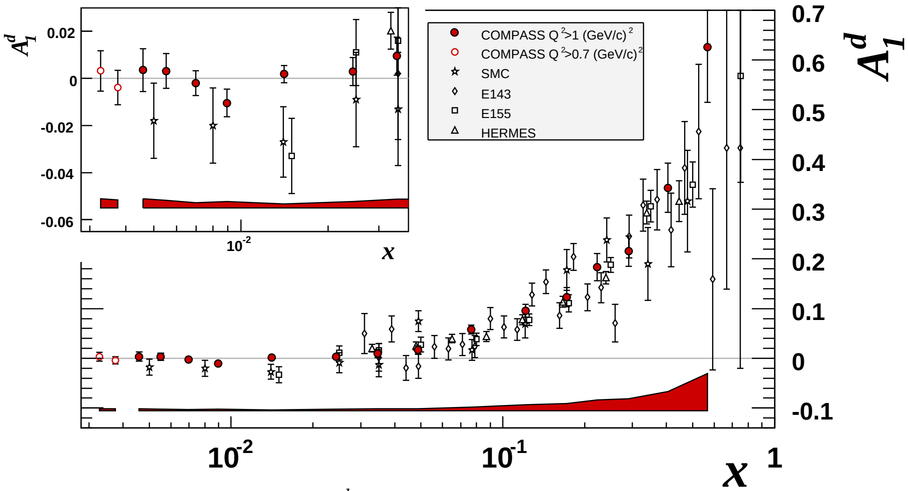

Figure 2: *The asymmetry $A_1^d(x)$ as measured by the world spin experiments. SLAC values of g_1/F_1 have been converted to A_1 and E155 data corresponding to the same x have been averaged over Q^2. The error bars are statistical. The shaded areas show the size of the COMPASS systematic errors; see text for details.*

precision of the COMPASS results [12] is considerably higher than the ones of SMC [15] and HERMES [16].

Figure 4 shows g_1^d, as a function of x for DIS events [13]. The SMC results [4] have evolved to the Q^2 of the corresponding COMPASS points. The two curves are the results of two QCD fits at the Q^2 of each data point. They are performed at NLO in the $\overline{\mathrm{MS}}$ renormalisation and factorisation scheme. These fits require input parameterisations of the quark singlet spin distribution $\Delta\Sigma(x)$, non-singlet distributions $\Delta q_3(x)$ and $\Delta q_8(x)$, and the gluon spin distribution $\Delta G(x)$, which evolve according to the DGLAP equations. They are written as:

$$\Delta F_k \;=\; \eta_k \frac{x^{\alpha_k}\,(1-x)^{\beta_k}\,(1+\gamma_k x)}{\int_0^1 x^{\alpha_k}\,(1-x)^{\beta_k}\,(1+\gamma_k x)dx}\,, \tag{4}$$

where ΔF_k represents each of the polarised parton distribution functions (PDF) and η_k is the integral of ΔF_k. The moments, η_k, of the non-singlet distributions Δq_3 and Δq_8 are fixed by the baryon decay constants (F+D) and (3F−D) respectively [17], assuming $\mathrm{SU}(3)_f$ flavour symmetry. The linear term $\gamma_k x$ is used only for the singlet distribution, in which case the exponent β_G is fixed

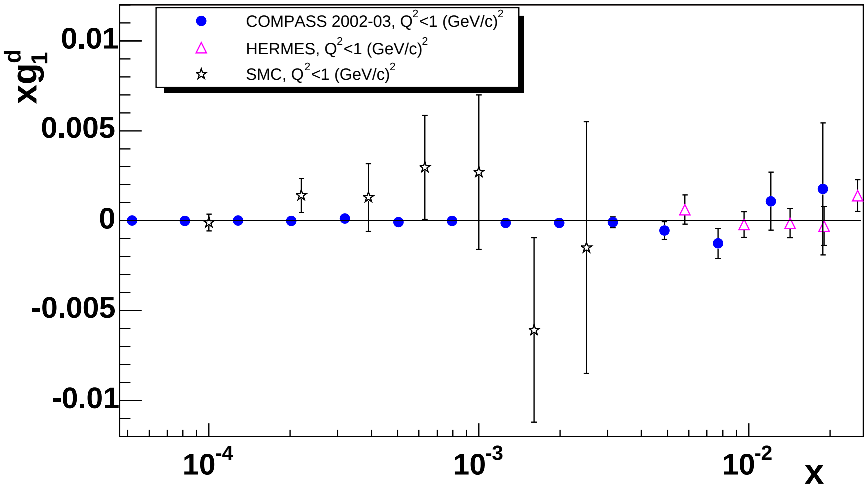

Figure 3: *The COMPASS [12], SMC [27] and Hermes [16] results for spin-dependent structure function of the deuteron, g_1^d, in the low x and low Q^2 region. The errors are statistical.*

because it is poorly constrained by the data; thus, 10 parameters are used in input distributions. Data are well described by two solutions of DGLAP, $\Delta G > 0$ and $\Delta G < 0$. Figure 5 shows the QCD fit to proton, deuteron and neutron targets, with positive ΔG solution (an indistinguishable curve is obtained for the solution with $\Delta G < 0$). All data have been evolved to a common Q_0^2 by means of the $g_1(x, Q^2)$ fitted parameterisation,

$$g_1(x, Q_0^2) = g_1(x, Q^2) + \left[g_1^{fit}(x, Q_0^2) - g_1^{fit}(x, Q^2)\right]. \quad (5)$$

We have used several fits of g_1 from the Durham data base [18]: Blümlein-Böttcher [19], GRSV [20] and LSS05 [21]. The value $Q_0^2 = 3\,(\mathrm{GeV}/c)^2$ has been chosen as reference because it is close to the average Q^2 of the COMPASS DIS data. The deuteron data are taken from Refs [4, 6, 8, 13, 14], the proton data from Refs [4, 6, 14, 22, 23] and the ^{3}He data from Refs [10, 24, 25, 26]. Concerning the COMPASS data in this fit, all x bins, except the last one, have been subdivided into three Q^2 intervals. The number of COMPASS data points used in the fit to deuteron data is 43, out of a total of 230. The resulting values of $g_1(x, Q^2)$ are calculated for the (x_i, Q_i^2) of each data point and compared to the experimental values. The parameters are found by minimizing the sum

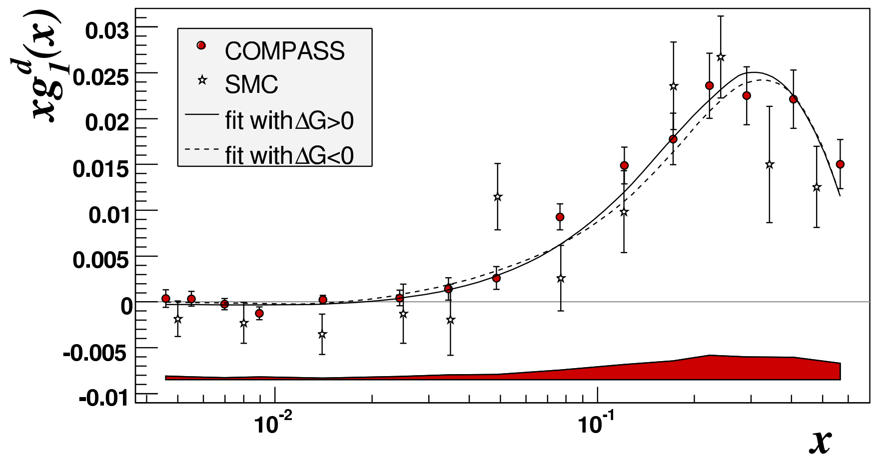

Figure 4: *The spin-dependent structure function of the deuteron, g_1^d, as a function of x ($Q^2 > 1\,(GeV/c)^2$). The COMPASS points are given at the $\langle Q^2 \rangle$ where they were measured. The SMC points have evolved to the Q^2 of the corresponding COMPASS points. Only statistical errors are shown. The shaded band stands for the COMPASS systematic error. The curves show the results of QCD fits with $\Delta G > 0$ and $\Delta G < 0$.*

$$\chi^2 = \sum_{i=1}^{N=230} \frac{\left[g_1^{fit}(x_i, Q_i^2) - g_1^{exp}(x_i, Q_i^2)\right]^2}{\left[\sigma(x_i, Q_i^2)\right]^2}\,, \tag{6}$$

where $\sigma(x_i, Q_i^2)$ are the statistical errors for all data sets, except for the proton data of E155 where the uncorrelated part of the systematic error on each point is added in quadrature to the statistical one. Two different programs have been used to fit the data – one uses the DGLAP evolution equations for the spin structure functions in x and Q^2 phase space [27)], the other uses the DGLAP evolution equations in the space of moments [28)]. Both programs give consistent values of the fitted PDF parameters and similar χ^2-probabilities. The polarised parton distributions for the three flavours and ΔG are shown in figure 6 for both $\Delta G < 0$ and $\Delta G > 0$ solutions. Quark distributions are weakly dependent on the sign of ΔG. Although the shapes of the gluon distributions differ over the whole x range, the fitted values of η_G are small and similar in absolute value $|\eta_G| \approx 0.2 - 0.3$. Similarly η_Σ reveals weak dependence on the shape of

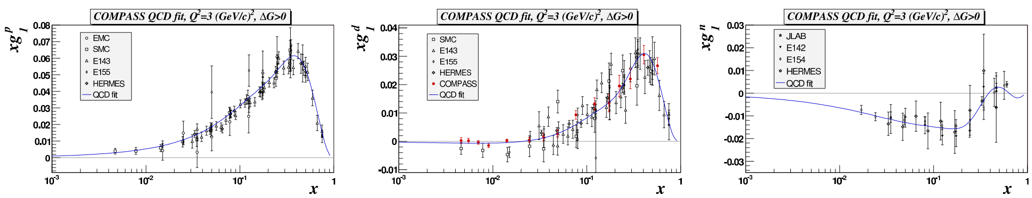

Figure 5: *The world data and QCD fit at* $Q^2 = 3\,GeV^2$*, obtained with the program of Ref.* [27]*. The curve corresponds to the solution with* $\Delta G > 0$*.*

ΔG, being slightly larger in the fit with $\Delta G < 0$. The results from the two fits have been averaged and give:

$$\eta_\Sigma(Q^2{=}3\,(\mathrm{GeV}/c)^2) \;=\; 0.30 \pm 0.01(stat.) \pm 0.02(evol.). \qquad (7)$$

In the $\overline{MS}$ scheme η_Σ is identical to the matrix element a_0, detailed below. More details on our QCD analysis can be found at Ref. [13].

The direct measurement of $\Delta G/G$, obtained at leading order in QCD, is compared with the indirect approach provided by the NLO QCD fits (figure 7). The unpolarised gluon distribution is taken from the MRST parametrisation [29]. The HERMES value [30] is positive and 2σ away from zero, whereas the preliminar one [31] is compatible with zero. The measured SMC point [32] is too imprecise to discriminate between positive or negative ΔG. Preliminar COMPASS points from measurements on high p_T hadron pairs [33] are consistent with both curves, whereas the value from the open charm channel is compatible with the $\Delta G < 0$ curve.

We have calculated the integral of g_1^N using exclusively the experimental values of COMPASS evolved to $Q_0^2 = 3$ GeV^2 and averaged over the two fits. Taking into account the contributions from the fits in the unmeasured regions of $x < 0.003$ and $x > 0.7$ we obtain:

$$\Gamma_1^N(Q^2{=}3\,(\mathrm{GeV}/c)^2) \;=\; 0.050 \pm 0.003(stat.) \pm 0.003(evol.) \pm 0.005(syst.). \quad (8)$$

The second error accounts for the difference in Q^2 evolution between the two fits. The systematic error is the dominant one and mainly corresponds to the uncertainty on the beam and target polarisations and on the dilution factor. One should notice that, taking into account only COMPASS data, the unmeasured regions contribute only with 2% to the integral of g_1^N.

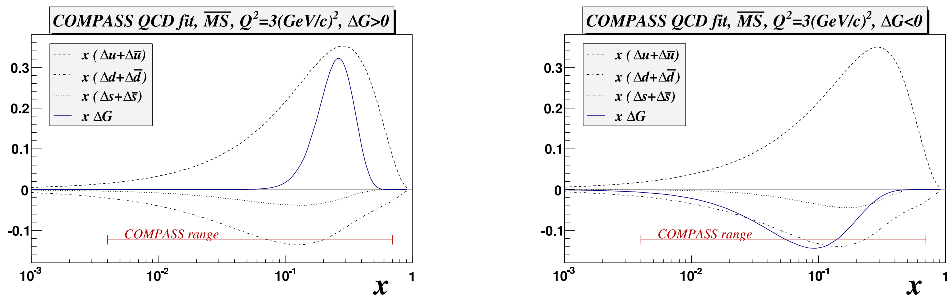

Figure 6: *Distributions* $x(\Delta u + \Delta\bar{u})$, $x(\Delta d + \Delta\bar{d})$, $x(\Delta s + \Delta\bar{s})$ *and* $x\Delta G$ *corresponding to the fits with* $\Delta G > 0$ *(left) and* $\Delta G < 0$ *(right) at* $Q^2 = 3$ *GeV*^{2}.

Γ_1^N is related to the matrix element of the singlet axial current a_0, which measures the quark spin contribution to the nucleon spin. The relation between Γ_1^N and a_0 in the limit $Q^2 \to \infty$ (Ref. [34]) is

$$\Gamma_1^N(Q^2) = \frac{1}{9}\,\hat{C}_1^S(Q^2)\,\hat{a}_0 \;+\; \frac{1}{36}\,C_1^{NS}(Q^2)\,a_8, \tag{9}$$

The coefficients $\hat{C}_1^S$ and C_1^{NS} have been calculated in perturbative QCD up to the third order in $\alpha_s(Q^2)$ [34]. From the COMPASS result of Eq. 8 and taking the value of a_8 measured in hyperon β decay, assuming $SU(3)_f$ flavour symmetry ($a_8 = 0.585 \pm 0.025$ [17]), one obtains:

$$\hat{a}_0 = 0.33 \pm 0.03(stat.) \pm 0.05(syst.), \tag{10}$$

with the value of α_s evolved from the PDG value $\alpha_s(\mathrm{M_z}^2) = 0.1187 \pm 0.005$. Combining this value with a_8, the first moment of the strange quark distribution is:

$$\Delta s(x) + \Delta\overline{s}(x) = \frac{1}{3}(\hat{a}_0 - a_8) = -0.08 \pm 0.01(stat.) \pm 0.02(syst.). \tag{11}$$

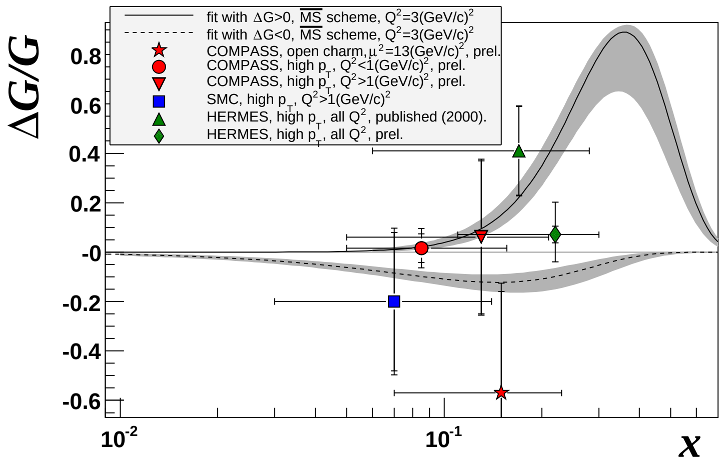

Figure 7: *Distribution of the gluon polarisation $\Delta G(x)/G(x)$ at $Q^2 = 3$ $(GeV/c)^2$ for the fits with $\Delta G > 0$ and $\Delta G < 0$ obtained with the program of Ref.* [27]*. The error bars associated to the points are statistical. The error bands correspond to the statistical error on $\Delta G(x)$ at a given x. The horizontal bar on each point shows the x-range of measurement.*

5 Conclusions

COMPASS has measured the deuteron spin asymmetry A_1^d and its longitudinal spin-dependent structure function g_1^d with improved precision at $Q^2 < 1$ $(\mathrm{GeV/c})^2$ and $0.0005 < x < 0.02$, as well as $1 < Q^2 < 100$ $(\mathrm{GeV/c})^2$ and $0.004 < x < 0.7$ $Q^2 > 1\,(\mathrm{GeV}/c)^2$. g_1^d is consistent with zero for $x < 0.03$. The measured values have been evolved to a common Q^2 by a NLO QCD fit of the world g_1 data. The fit yields two solutions, one corresponding to $\Delta G(x) > 0$ and other to $\Delta G(x) < 0$, which describe the data equally well. Although the shapes of the distributions are very different, their absolute values of the first moment of $\Delta G(x)$ are similar and not larger than 0.3. Taking into account only COMPASS data the first moment Γ_1^N has been evaluated at $Q^2 = 3$ $(\mathrm{GeV}/c)^2$ with a statistical error of about 6%. From this integral the matrix element of the singlet axial current $\hat{a}_0$ in the limit $Q^2 \to \infty$ is extracted. At the order α_s^3, it has been found $\hat{a}_0 = 0.33 \pm 0.03(stat.) \pm 0.05(syst.)$.

Acknowledgments

This work was partially supported by Fundação para a Ciência e a Tecnologia – Portugal.

References

1. M.J. Alguard *et al.* (E80 Coll.), Phys. Rev. Lett. **37**, 1261 (1976).
2. J.R. Ellis and R.L. Jaffe, Phys. Rev. D **9**, 1444 (1974).
3. J. Ashman *et al.* (EMC Coll.), Phys. Lett. B **206**, 364 (1988).
4. B. Adeva *et al.* (SMC Coll.), Phys. Rev. D **58**, 112001 (1998).
5. P.L. Anthony *et al.* (E142 Coll.), Phys. Rev. D **54**, 6620(1996).
6. K. Abe *et al.* (E143 Coll.) Phys. Rev. D **58**, 112003 (1998).
7. K. Abe *et al.* (E154 Coll.), Phys. Lett. B **405**, 180 (1997).
8. P. L. Anthony *et al.,* (E155 Coll.) Phys. Lett. B **463**, 339 (1999).
9. A. Airapetian *et al.* (HERMES Coll.), Phys. Lett. B **442**, 484 (1998).
10. X. Zheng *et al.* (JLAB/Hall A Coll.), Phys. Rev. Lett. **92** 012004 (2004).
11. P. Abbon *et al.* (COMPASS Coll.), CERN-PH-EP/2007-001, hep-ex/0703049. *To be published in Nucl. Inst. and Meths.*
12. V.Yu. Alexakhin *et al.* (COMPASS Coll.), Phys. Lett. B **647**, 330 (2007).
13. V.Yu. Alexakhin *et al.* (COMPASS Coll.), Phys. Lett. B **647**, 8 (2007).
14. A. Airapetian *et al.* (HERMES Coll.), Phys. Rev. D **75**, 012003 (2005)
15. B. Adeva *et al.* (SMC Coll.), Phys. Rev. D **60** 072004 (1999); erratum *ibid.* **62** 079902 (2000).
16. A. Airapetian *et al.* (HERMES Coll.), Phys. Rev. D **75** 012007 (2007).
17. Y. Goto *et al.*, Phys. Rev. D **62**, 037503 (2003).
18. The Durham HEP Databases, http://durpdg.dur.ac.uk/HEPDATA/pdf.html

19. J. Blümlein and H. Böttcher, Nucl. Phys. B **636**, 225 (2002).

20. M. Glück, E. Reya, M. Stratmann and W. Vogelsang, Phys. Rev. D **63**, 094005 (2001).

21. E. Leader, A. V. Sidorov and D. B. Stamenov, Phys. Rev. D **73** 034023 (2006).

22. P. L. Anthony *et al.* (E155 Coll.), Phys. Lett. B **493**, 19 (2000).

23. J. Ashman *et al.* (EMC Coll.), Nucl. Phys. B **328** (1989).

24. P. L. Anthony *et al.* (E142 Coll.), Phys. Rev. D **54**, 6620 (1996).

25. K. Abe *et al.* (E154 Coll.), Phys. Rev. Lett. **79**, 26 (1997).

26. K. Ackerstaff *et al.* (HERMES Coll.), Phys. Lett. B **404**, 383 (1997).

27. B. Adeva *et al.* (SMC Coll.), Phys. Rev. D **58** 112002 (1998).

28. A. N. Sissakian, O. Yu. Shevchenko and O. N. Ivanov, Phys. Rev. D **70**, 074032 (2004).

29. A. D. Martin, R. G. Roberts, W. J. Stirling and R. S. Thorne, Eur. Phys. J. C **4**, 463 (1998).

30. A. Airapetian *et al.,* (HERMES Coll.), Phys. Rev. Lett. **84**, 2584 (2000).

31. D. Hasch (HERMES Coll.), AIP Conf. Proc. **915**, 307 (2006).

32. B. Adeva *et al.,* (SMC Coll.), Phys. Rev. D **70**, 012002 (2004).

33. E. S. Ageev *et al.,* (COMPASS Coll.), Phys. Lett. B **633**, 25 (2006).

34. S. A. Larin *et al.*, Phys. Lett. B **404**, 153 (1997).